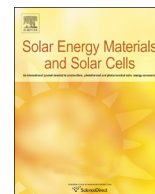




ELSEVIER

Contents lists available at ScienceDirect

Solar Energy Materials & Solar Cells

journal homepage: www.elsevier.com/locate/solmat

Performance evaluation of a GaInP/GaAs solar cell structure with the integration of AlGaAs tunnel junction

Yunus Özen^{a,b,*}, Nihan Akın^{a,b}, Barış Kınacı^c, Süleyman Özçelik^{a,b}^a Photonics Application and Research Center, Gazi University, 06500 Ankara, Turkey^b Department of Physics, Faculty of Science, Gazi University, 06500 Ankara, Turkey^c Department of Physics, Faculty of Science, Istanbul University, 34134 Vezneciler Istanbul, Turkey

ARTICLE INFO

Article history:

Received 12 December 2014

Received in revised form

28 December 2014

Accepted 13 January 2015

Keywords:

GaInP/GaAs solar cell

AlGaAs tunnel junction

The energy conversion efficiency

ABSTRACT

A GaInP/GaAs solar cell structure with AlGaAs tunnel junction was grown on p-type (1 0 0)-oriented GaAs substrate by a solid-source molecular beam epitaxy technique. The structural and morphological properties of the GaInP/GaAs solar cell structure have been evaluated by means of secondary ion mass spectrometry and atomic force microscopy measurements. In addition, the GaInP/GaAs solar cell device was fabricated to obtain electrical output parameters of the cells. For this purpose, the current–voltage measurements of solar cell devices were carried out at room temperature under both dark and air mass 1.5 global radiation (AM1.5) using solar simulator. In addition, the electrical output parameters of the GaInP/GaAs solar cell structure with the AlGaAs tunnel junction are compared with the GaInP/GaAs solar cell structure without the AlGaAs tunnel junction, and it is found that the integration of the tunnel junction into a solar cell structure improves the device performance by 48%.

© 2015 Elsevier B.V. All rights reserved.

1. Introduction

According to literature, solar cells (SCs) can be divided into four groups: (1) silicon-based SCs such as mono-crystalline silicon, and poly-crystalline silicon SCs [1–7], (2) thin film SCs such as amorphous silicon, cadmium–telluride, and copper–indium–gallium–de selenide SCs [8–15], and (3) III–V group SCs such as quantum well, and multi-junction SCs [16–29], (4) other SCs such as organic, dye sensitized and perovskite SCs [30–33]. There has been an increasing interest on the research and development of multi-junction III–V group SCs due to a higher efficiency compared to other groups SCs. Currently, the studies on these SCs are mainly focused on the performance evaluation [34–38]. Multi-junction SCs are sensitive to radiation of different wavelengths. A top cell is responsive to shorter wavelengths, whereas a bottom cell is responsive to longer wavelengths. In configuration, wider bandgap materials are used for the top cells since they absorb short wavelengths. Thus, it allows the longer wavelength radiation to penetrate deeper into the device where it can be converted into electrical energy. The commonly used highest-performing multi-junction cells use III–V compound semiconductors with direct

bandgaps [39]. III–V Group ternary alloy materials, such as AlGaAs, InGaAs, InGaN and GaInP, were widely used as the top cell of SCs [18,20,22,25,27,29,34–38]. Among these materials, GaInP ternary alloy is an essential material for high efficiency SCs as it absorbs the visible part of the solar spectrum [40]. In addition, GaAs binary compound (bandgap: 1.42 eV) absorbs near-infrared part of the solar spectrum. When the Ga composition ratio is approximately 51% of the GaInP/GaAs structure, GaInP ternary alloy grows on a GaAs substrate with lattice-match, and this structure has great technological importance [40–42]. The GaInP/GaAs SC structure will continue to be the focus of attention in the photovoltaic works as it absorbs the large part of the solar spectrum.

Tunnel junctions (TJs) are highly doped p–n diodes which allow for quantum mechanical tunneling through their narrow depletion regions. TJs are very crucial for multi-junction SCs, and they have properties such as a relatively optically transparent and low resistance [43]. According to the tunneling effect, the electron does not need extra energy for tunneling from the bottom of the conduction band to the top of the valence band. In addition, heavily doped AlGaAs, InGaP, GaAs, etc. are selected as TJs in III–V group SCs [27]. Several researches have studied the SCs structure with an integration of TJ [27,28,34]. Siyu et al. [27] examined the characteristics of the TJ, the material used in the TJ, the compensation of the TJ to the overall cell's characteristics, the TJs' influence on the current density of sub-cells and the efficiency increase. Wheelden et al. [28] investigated four different TJ designs

* Corresponding author at: Photonics Application and Research Center, Gazi University, 06500 Ankara, Turkey. Tel.: +90 312 202 12 79; fax: +90 312 212 22 79.
E-mail addresses: ynszn.gazi@gmail.com, sozcelik@gazi.edu.tr (Y. Özen).

(AlGaAs/AlGaAs, GaAs/GaAs, AlGaAs/InGaP, AlGaAs/GaAs) for multi-junction SCs under high concentration to determine the peak tunneling current and resistance change as a function of the doping concentration. They clearly demonstrated that the advantages of the AlGaAs/GaAs and the AlGaAs/AlGaAs TJ design more than the GaAs/GaAs and the AlGaAs/InGaP TJ design. Samberg et al. [34] investigated the effect of the heterojunction interface on the performance of high bandgap InGaP:Te/AlGaAs:C TJs and the compared experimental results with the modeling results are reasonable. They showed that the high tunneling current achieved in these TJs with a voltage drop of only a few mV across the junction can allow multi-junction SCs to operate at higher concentrations. As a result, TJ plays a crucial role in the multi-junction cell design, and they have an essential impact on the performance and reliability of the devices.

In our previous study [37], the GaInP/GaAs SC structure was grown using the molecular beam epitaxy (MBE) technique. We investigated the structural, optical and morphological properties of GaInP/GaAs solar cell (SC) structure, and we also obtained the energy conversion efficiency value as 9.13%. In the light of our previous study, the purpose of this research is to examine the effect of AlGaAs TJ on the cell's electrical output parameters of the

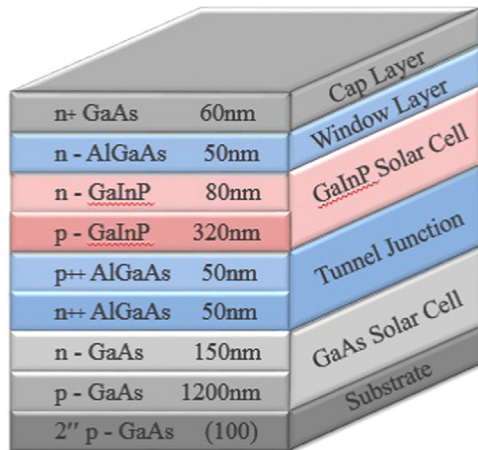


Fig. 1. The schematic diagram of the solar cell structure.

GaInP/GaAs SC structure. Thus, this paper is organized as follows: the GaInP/GaAs SC structure was grown on p-type (1 0 0)-oriented GaAs substrate by MBE. The secondary ion mass spectrometry (SIMS) measurement was preferred to analyze the depth profile of the GaInP/GaAs SC structure. Thus, not only main elements (Ga, In, Al, As and P) were detected, but also dopant elements (Si and Be) in the epi-layer. The morphology and the surface roughness were determined using atomic force microscopy (AFM) measurements. In addition, device parameters such as open-circuit voltage (V_{oc}), short-circuit current (I_{sc}), fill factor (FF) and energy conversion efficiency (η) of GaInP/GaAs SC structure with AlGaAs TJ were extracted from the current–voltage (I – V) characteristics.

2. Experimental method

The GaInP/GaAs SC structure was grown on a p-type (1 0 0)-oriented GaAs substrate using a V80H solid source MBE system. Prior to the growth process, the GaAs substrate was chemically cleaned. After the cleaning process, first a 1.2 μm thick p-GaAs layer was grown on the substrate at about substrate temperature of $T_s=650$ °C and then 150 nm thick n-GaAs (bottom cell) was grown at $T_s=640$ °C. After then 50 nm thick n++AlGaAs and 50 nm thick p++AlGaAs were grown at the same temperature from the AlGaAs tunnel junction. Then 320 nm thick p-GaInP and 80 nm thick n-GaInP (top cell) were grown using a GaP decomposition source at $T_s=530$ °C, respectively. The solar cell structure was completed by a growth of a 50 nm thick n-AlGaAs window layer and a 60 nm thick n-GaAs layer. Si and Be were incorporated as an n-type and p-type dopant, respectively. The schematic diagram of the solar cell structure is represented in Fig. 1. The reconstruction of the epi-surfaces and growth rate were determined using reflection high energy electron diffraction (RHEED) oscillations.

Atomic distributions and interface characteristics of the GaInP/GaAs SC structure were performed by SIMS (Hiden Analytical Ltd., Warrington, UK) depth profile measurements. The SIMS measurements were carried out with an O_2 (oxygen) gun set at an ion energy of 5 keV and with a detector sensitivity of 400 nA/V. During the SIMS experiments, base pressure of the chamber was kept at 10^{-10} mbar.

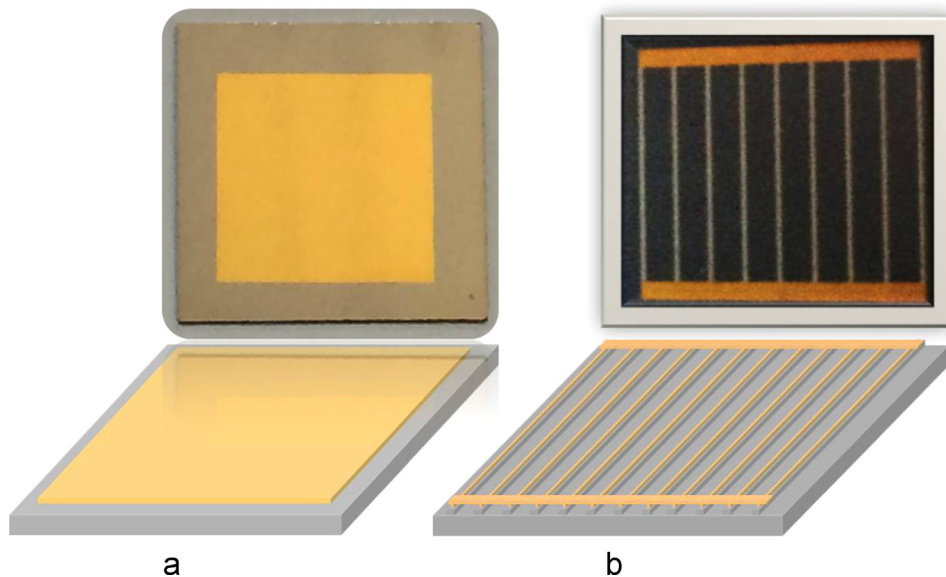


Fig. 2. (a) The back metal pad patterning, (b) the front metal pad patterning.

Morphological properties of the GaInP/GaAs SC structure were characterized at room temperature (RT) using high performance AFM (Nano Magnetics Instruments Ltd., Oxford, UK) using dynamic mode scanning. The scan area was set as $5 \times 5 \mu\text{m}^2$, and the scan rate was 2 Hz (using a resolution of 256 lines per scan).

For the electrical characterization of the GaInP/GaAs SC structure, first the back contact was formed. For the back metal pad patterning, photolithography process was done using square (0.64 cm^2) mask and the schematic diagram is represented in Fig. 2a. The metallization was then completed by deposition of high purity Au (99.999%) using thermal evaporation system with 10^{-8} mbar base pressure. For the front metal pad patterning, photolithography process was done using mask, and the schematic diagram is represented in Fig. 2b, and the metalization was completed by deposition of high purity Au (99.999%). As a last step of the fabrication process, the GaInP/GaAs SC was annealed via rapid thermal annealing during 60 s at 400°C to form ohmic metallization. The photolithography process was performed using Kalr-Suss MJB4 mask aligner system, and the current–voltage characteristics were performed using Keithley 4200 source-meter and Oriel Sol1A class AAA solar simulator.

3. Results and discussion

In this work, we have investigated the performance evaluation of the GaInP/GaAs solar cell structure with the integration of AlGaAs tunnel junction. The performance of the solar cell structures significantly depends on the atomic homogeneity in the grown layers and interface characteristics. Thus, SIMS is an important and widely used analytical technique in semiconductor device structures such as SCs to examine dopant profiling within a patterned junction or contact. Therefore, SIMS analysis was performed to investigate layer-by-layer growth mode of the GaInP/GaAs SC structure. Although the reference sample was not used to calculate concentrations of the dopant elements (Si and Be), their dispersions in the layers were successfully determined from the SIMS depth profile, as seen in Fig. 3. In addition, achievement of desired 100 nm thick AlGaAs TJ between top n-GaInP and bottom n-GaAs cells can be clearly seen from Fig. 4.

Fig. 5a and b shows that two-dimensional (2D) and three-dimensional (3D) AFM images with a $5 \times 5 \mu\text{m}^2$ scan area of the GaInP/GaAs SC structure, respectively. The SC structure has a very uniform surface morphology with root mean square (RMS) roughness of 1.75 nm (given in Table 1) without any surface cracks or

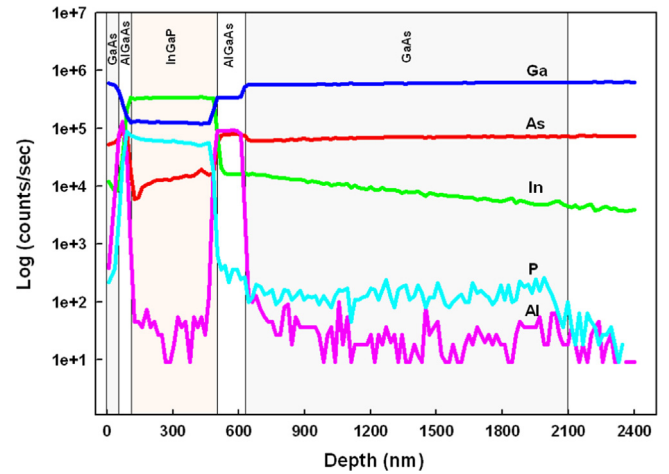


Fig. 4. SIMS depth profile of the GaInP/GaAs SC structure.

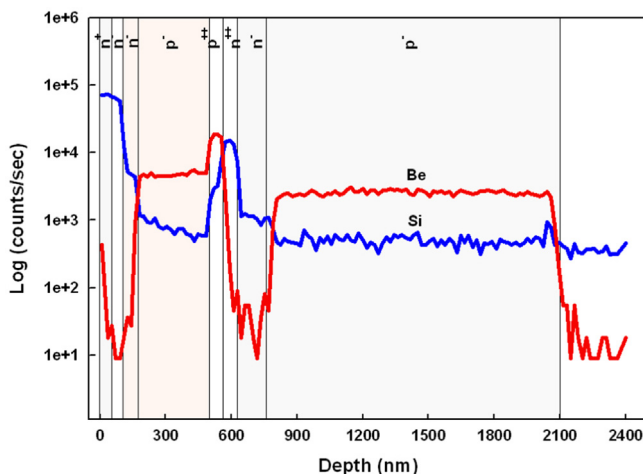


Fig. 3. Dispersions of the dopant elements (Si and Be) in the layer.

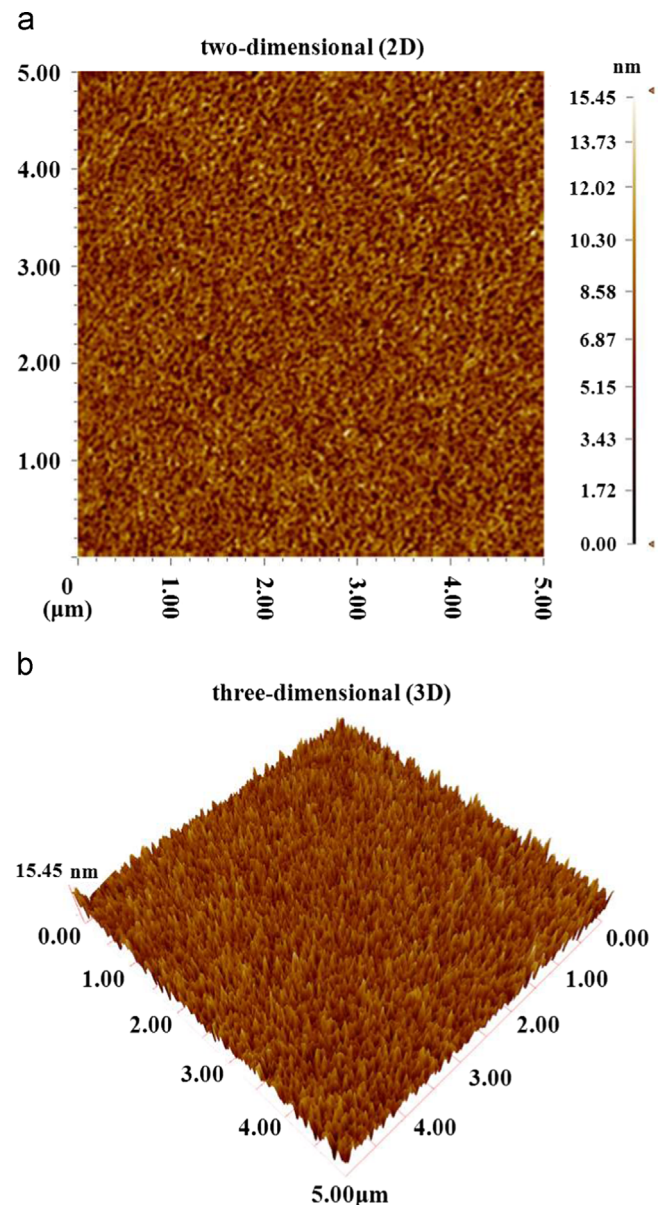


Fig. 5. (a) Two- and (b) three-dimensional AFM images ($3 \mu\text{m}^2$) showing the surface morphology of a GaInP/GaAs SC structure.

Table 1
Experimental values of device parameters comparison with Ref. [37].

Parameter	[37] ^a	This work ^b
RMS (nm)	0.99	1.75
V_{oc} (V)	0.50	1.38
I_{sc} (mA)	2.07	13.43
FF	0.67	0.62
η (%)	9.13	13.52

RMS—root mean square. V_{oc} —open-circuit voltage. I_{sc} —short-circuit current. FF—fill factor. H —energy conversion efficiency.

^a GaInP/GaAs solar cell without AlGaAs tunnel junction.

^b GaInP/GaAs solar cell with AlGaAs tunnel junction.

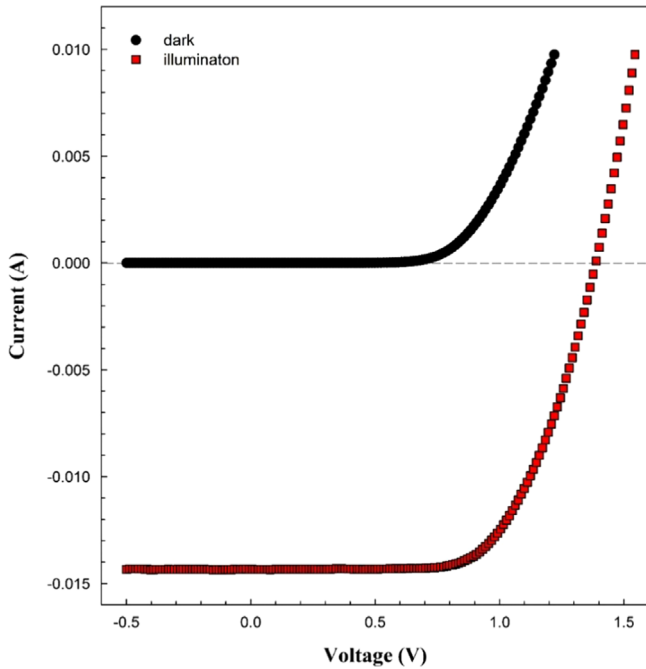


Fig. 6. The current–voltage characteristic of the GaInP/GaAs SC structure at room temperature under both dark air mass 1.5 global radiation (AM1.5G).

defects. It is well known that RMS roughness is effective on efficiency of the SC structure, and the device efficiency increases with increasing the RMS value as emphasized in our previous study [37].

After the completion of the structural and morphological characterizations, the electrical characterization was done at room temperature, and I – V characteristic was shown in Fig. 6. The overall solar energy to electricity conversion efficiency of a solar cell is defined as the ratio of the maximum output of the cell divided by the power of incident light. It can be determined by the V_{oc} , I_{sc} , FF, and the intensity of the incident light (P_{in}) as shown in Eq. (1). Since it is dependent on all the three first factors under standard conditions, it is of great importance to optimize each one of them for high overall efficiency [44].

$$\eta = \frac{P_{out}}{P_{in}} = \frac{I_{sc} \times V_{oc} \times FF}{P_{in}} \quad (1)$$

where V_{oc} , I_{sc} , FF and η values of the GaInP/GaAs SC structure with the AlGaAs TJ are given in Table 1 compared with Ref. [37]. When we compare these results with our previous study, both the integration of the TJ into the SC structure and increasing the RMS value improves the device performance by 48%.

4. Conclusion

In this work, we report the growth, characterizations and fabrication of the GaInP/GaAs SC structure with the AlGaAs TJ. Lattice-match GaInP/GaAs SC structure was successfully grown by solid source MBE with a GaP decomposition source. The structural characterization was done using SIMS, and it was found that AlGaAs TJ between top n-GaInP and bottom n-GaAs cells with the desired thickness of 100 nm was achieved. The morphological characterization was done using AFM, and it was found defects on surface, and crack-free uniform surface morphology could be achieved. At last, the SC device was fabricated using photolithography, and electrical characterization was performed under both and air mass 1.5 global radiation (AM1.5G) using a solar simulator, and it was found that the integration of AlGaAs TJ increases the efficiency of the SC structure by 48%. According to experimental results, the integration of TJ is very effective on device performance, and the SC structure having AlGaAs TJ can be a promising candidate to be used as a photovoltaic device.

Acknowledgements

This work is supported by the Ministry of Development of Turkey (2011K120290), the Ministry of Science, Industry and Technology of Turkey (SANTEZ-00587.STZ.2010-1), the Ministry of Science, Industry and Technology of Turkey (0254.TGSD.2014) and TUBITAK under Project No. 118T333.

References

- [1] C.S. Solanki, L. Cornel, K.V. Nieuwenhuysen, A. Ulyashin, N. Posthuma, G. Beaucarne, J. Poortmans, Thin film free-standing monocrystalline Si solar cells with heterojunction emitter, *Prog. Photovoltaics* 13 (2005) 201–208.
- [2] I. Gordon, S. Vallon, A. Nayolet, G. Beaucarne, J. Poortmans, Thin-film monocrystalline-silicon solar cells made by a seed layer approach on glass-ceramic substrate, *Sol. Energy Mater. Sol. Cells* 94 (2010) 381–385.
- [3] G. Yang, Rene A.C.M.M. van Swaaij, H. Tan, O. Isabella, M. Zeman, Modulated surface textured glass as substrate for high efficiency microcrystalline silicon solar cells, *Sol. Energy Mater. Sol. Cells* 133 (2015) 156–162.
- [4] A. Slaoui, S. Bourdais, G. Beaucarne, J. Poortmans, S. Reber, Polycrystalline silicon solar cells on mullite substrates, *Sol. Energy Mater. Sol. Cells* 71 (2002) 245–252.
- [5] A.G. Aberle, A. Straub, P.I. Widenborg, A.B. Sproul, Y. Huang, P. Campbell, Polycrystalline silicon thin-film solar cells on glass by aluminium-induced crystallisation and subsequent ion-assisted deposition (ALICIA), *Prog. Photovoltaics* 13 (2005) 37–47.
- [6] I. Gordon, L. Cornel, D.V. Gestel, G. Beaucarne, J. Poortmans, 8% Efficient thin-film polycrystalline-silicon solar cells based on aluminum-induced crystallization and thermal CVD, *Prog. Photovoltaics* 15 (2007) 575–586.
- [7] P. Yadav, B. Tripathi, K. Pandey, M. Kumar, Investigating the charge transport kinetics in-poly-crystalline silicon solar cells for low-concentration illumination by impedance spectroscopy, *Sol. Energy Mater. Sol. Cells* 133 (2015) 105–112.
- [8] M. Schmidt, L. Korte, A. Laades, R. Stongl, Ch. Schubert, H. Angermann, E. Conrad, K. Maydell, Physical aspects of a-Si:H/c-Si hetero-junction solar cells, *Thin Solid Films* 515 (2007) 7475–7480.
- [9] J.W. Schüttauf, B. Niesen, L. Löfgren, M. Bonnet-Eymard, M. Stuckelberger, S. Hanni, M. Boccard, G. Bugnon, M. Despeisse, F.J. Haug, F. Meillaud, C. Ballif, Amorphous silicon-germanium for triple and quadruple junction thin-film silicon based solar cell, *Sol. Energy Mater. Sol. Cells* 133 (2015) 163–169.
- [10] X. Wu, High-efficiency polycrystalline CdTe thin-film solar cells, *Sol. Energy* 77 (2004) 803–814.
- [11] J. Sites, J. Pan, Strategies to increase CdTe solar-cell voltage, *Thin Solid Films* 515 (2007) 6099 (6012).
- [12] J. Li, D.R. Diercks, T.R. Ohno, C.W. Warren, M.C. Lonergan, J.D. Beach, C.A. Wolden, Controlled activation of ZnTe:Cu contacted CdTe solar cell using rapid thermal processing, *Sol. Energy Mater. Sol. Cells* 133 (2015) 208–215.
- [13] D. Rudmann, D. Bremoud, H. Zogg, A.N. Tiwari, Na incorporation into Cu(In, Ga) Se₂ for high-efficiency flexible solar cells on polymer foils, *J. Appl. Phys.* 97 (2005) 084903.
- [14] M.M. Islam, S. Ishizuka, A. Yamada, K. Sakurai, S. Niki, T. Sakurai, K. Akimoto, CIGS solar cell with MBE-grown ZnS buffer layer, *Sol. Energy Mater. Sol. Cells* 93 (2009) 970–972.
- [15] J. Chantana, D. Hironiwa, T. Watanabe, S. Teraji, K. Kawamura, T. Minemoto, Controlled back slope of Ga/(In+Ga) profile in Cu(In,Ga)Se₂ absorber

- fabricated by multi layer precursor method for improvement of its photovoltaic performance, *Sol. Energy Mater. Sol. Cells* 133 (2015) 223–228.
- [16] R. Dahal, J. Li, K. Aryal, J.Y. Lin, H.X. Jinang, InGaN/GaN multiple quantum well concentrator solar cell, *Appl. Phys. Lett.* 97 (2010) 073115.
- [17] K.W.J. Barnham, I. Ballard, J.P. Connolly, N.J. Ekins-Daukes, B.G. Kluftinger, J. Nelson, C. Rohr, Quantum well solar cells, *Physica E* 14 (2002) 27–36.
- [18] G.F. Virshup, C.W. Ford, J.G. Werthen, A 19% efficient AlGaAs solar cell with graded band gap, *Appl. Phys. Lett.* 47 (1985) 1319–1321.
- [19] H. Sugiura, C. Amano, A. Yamamoto, M. Yamaguchi, Double heterostructure GaAs tunnel junction for a AlGaAs/GaAs tandem solar cell, *Jpn. J. Appl. Phys.* 27 (1988) 269–272.
- [20] J.M. Zahler, K. Tanabe, C. Ladous, T. Pinnington, F.D. Newman, H.A. Atwater, High efficiency InGaAs solar cells on Si by InP layer transfer, *Appl. Phys. Lett.* 91 (2007) 012108.
- [21] O. Jani, I. Ferguson, C. Honsberg, S. Kurtz, Design and characterization of GaN/InGaN solar cells, *Appl. Phys. Lett.* 91 (2007) 132117.
- [22] R. Dahal, B. Pantha, J. Li, J.Y. Lin, H.X. Jiang, InGaN/GaN multiple quantum well solar cells with long operating wavelengths, *Appl. Phys. Lett.* 94 (2009) 063505.
- [23] E. Matioli, C. Neufeld, M. Iza, S.C. Cruz, A.A. Al-Hejji, X. Chen, R.M. Farrell, S. Keller, S. DenBaars, U. Mishra, S. Nakamura, J. Speck, C. Weisbuch, *Appl. Phys. Lett.* 98 (2011) 021102.
- [24] M. Yamaguachi, T. Takamoto, K. Araki, N.J. Ekins-Daukes, Multi-junction III–V solar cells: current status and future potential, *Sol. Energy* 79 (2005) 78–85.
- [25] W. Guter, J. Schöne, S.P. Philipps, M. Steiner, G. Siefert, A. Wekkeli, E. Welsler, E. Oliva, A.W. Bett, F. Dimroth, Current-matched triple-junction solar cell reaching 41.1% conversion efficiency under concentrated sunlight, *Appl. Phys. Lett.* 94 (2009) 223504.
- [26] D.C. Law, R.R. King, H. Yoon, M.J. Archer, A. Boca, C.M. Fetzer, S. Mesropian, T. Isshiki, M. Haddad, K.M. Edmondson, D. Bhusari, J. Yen, R.A. Sherif, H. A. Atwater, N.H. Karam, Future technology pathways of terrestrial III–V multijunction solar cells for concentrator photovoltaic systems, *Sol. Energy Mater. Sol. Cells* 94 (2010) 1314–1318.
- [27] L. Siyu, Q. Xiaosheng, AlGaAs/GaAs tunnel junction in a 4-J tandem solar cell, *J. Semicond.* 32 (2011) 112003.
- [28] J.F. Wheelden, C.E. Valdivia, A.W. Walker, G. Kolhatkar, A. Jaouad, A. Turala, B. Riel, D. Masson, N. Puetz, S. Fafard, R. Ares, V. Aimez, T.J. Hall, K. Hiazer, Performance comparison of AlGaAs, GaAs and InGaP tunnel junctions for concentrated multijunction solar cells, *Prog. Photovoltaics* 19 (2011) 442–452.
- [29] M. Yamaguachi, Japanese R&D activities of high efficiency III–V compound multi-junction and concentrator solar cell, *Energy Procedia* 15 (2012) 265–274.
- [30] J.C. Ke, Y.H. Wang, K.L. Chen, C.J. Huang, Effect of open-circuit voltage in organic solar cells based on various electron donor materials by inserting molybdenum trioxide anode buffer layer, *Sol. Energy Mater. Sol. Cells* 133 (2015) 248–254.
- [31] S. Mathew, A. Yella, P. Gao, R. Humphry-Baker, B.F.E. Curchad, N. Ashari-Astani, I. Tavernelli, U. Rothlisberger, Md.K. Mazeruddin, M. Gratzel, Dye-sensitized solar cells with 13% efficiency achieved through the molecular engineering of porphyrin sensitizers, *Nat. Chem.* 6 (2014) 242–247.
- [32] T. Minemoto, M. Murata, Theoretical analysis on effect of band offsets in perovskite solar cells, *Sol. Energy Mater. Sol. Cells* 133 (2015) 8–14.
- [33] S. Senthilarasu, E.F. Fernandez, F. Almonacid, T.K. Mallick, Effects of spectral coupling on perovskite solar cells under diverse climatic conditions, *Sol. Energy Mater. Sol. Cells* 133 (2015) 92–98.
- [34] J.P. Samberg, C.Z. Carlin, G.K. Bradshaw, P.C. Colter, J.L. Harmon, J.B. Allen, J.R. Hauser, S.M. Bedair, Effect of GaAs interfacial layer on the performance of high bandgap tunnel junctions for multijunction solar cells, *Appl. Phys. Lett.* 103 (2013) 103503.
- [35] M. Lu, R. Wang, Y. Liu, Z. Feng, Z. Han, C. Hou, Displacement damage dose approach to predict performance degradation of on-orbit GaInP/GaAs/Ge solar cells, *Nucl. Instrum. Methods Phys. Res. B* 307 (2013) 362–365.
- [36] J.F. Geisz, M.A. Steiner, I. Garcia, S.R. Kurtz, D.J. Friedman, Enhanced external radiative efficiency for 20.8% efficient single-junction GaInP solar cells, *Appl. Phys. Lett.* 103 (2013) 041118.
- [37] B. Kinaci, Y. Özen, T. Asar, S.Ş. Çetin, T. Memmedli, M. Kasap, S. Özçelik, Study on growth and characterizations of $\text{Ga}_x\text{In}_{1-x}\text{P}/\text{GaAs}$ solar cell structure, *J. Mater. Sci. Mater. Electron.* 24 (2013) 3269–3274.
- [38] G.M.M.W. Bissels, M.A.H. Asselbergs, J.M. Dickhout, E.J. Haverkamp, P. Mulder, G.J. Bauhuis, E. Vlieg, J.J. Schermer, Experimental review of series resistance determination methods for III–V concentrator solar cells, *Sol. Energy Mater. Sol. Cells* 130 (2014) 364–374.
- [39] M. Cooke, Moving forward from 44% to 50% conversion for III–V solar cells, technology focus: photovoltaics, *Compd. Adv. Silicon* 7 (2013) 72–77.
- [40] R. Ferrini, G. Guizzetti, M. Patrini, A. Parisini, L. Tarricone, B. Valenti, Optical functions of InGaP/GaAs epitaxial layers from 0.01 to 5.5 eV, *Eur. Phys. J. B* 27 (2002) 449–458.
- [41] S. Mangal, P. Ghelfi, A. Bogoni, P. Banerji, Barrier height dependence of Fano factor and $1/f$ noise effect on InGaP based Schottky barrier diode, *J. Appl. Phys.* 110 (2011) 033721.
- [42] B. Kinaci, Y. Özen, K. Kızılkaya, T. Asar, S.Ş. Çetin, E. Boyalı, M.K. Öztürk, T. Memmedli, S. Özçelik, Effect of alloy composition on structural, optical and morphological properties and electrical characteristics of $\text{Ga}_x\text{In}_{1-x}\text{P}/\text{GaAs}$ structure, *J. Mater. Sci. Mater. Electron.* 24 (2013) 1375–1381.
- [43] A. Sharenko, Optimization of tunnel diodes in multi-junction solar cells, the 2009 NNIN REU research accomplishments, *Electronics* (2009) 60–61.
- [44] K.M. Karlsson, Design, Synthesis and Properties of Organic Sensitizers for Dye Sensitized Solar Cells (Doctoral Thesis), KTH Chemical Science and Engineering, royal Institute of Technology, Stockholm, Sweden, 2011.